## LETTERS

# Solar radiation and functional traits explain the decline of forest primary productivity along a tropical elevation gradient

Nikolaos M. Fyllas,[1*]
Lisa Patrick Bentley,[1]
Alexander Shenkin,[1]
Gregory P. Asner,[2] Owen K. Atkin,[3]
Sandra Díaz,[4] Brian J. Enquist,[5,6]
William Farfan-Rios,[7]
Emanuel Gloor,[8]
Rossella Guerrieri,[9,10]
Walter Huaraca Huasco,[11]
Yoko Ishida,[12]
Roberta E. Martin,[2] Patrick Meir,[10,13]
Oliver Phillips,[8] Norma Salinas,[1,14]
Miles Silman,[7]
Lasantha K Weerasinghe,[13,15]
Joana Zaragoza-Castells[13,16] and
Yadvinder Malhi[1]

**Abstract**

One of the major challenges in ecology is to understand how ecosystems respond to changes in environmental conditions, and how taxonomic and functional diversity mediate these changes. In this study, we use a trait-spectra and individual-based model, to analyse variation in forest primary productivity along a 3.3 km elevation gradient in the Amazon-Andes. The model accurately predicted the magnitude and trends in forest productivity with elevation, with solar radiation and plant functional traits (leaf dry mass per area, leaf nitrogen and phosphorus concentration, and wood density) collectively accounting for productivity variation. Remarkably, explicit representation of temperature variation with elevation was not required to achieve accurate predictions of forest productivity, as trait variation driven by species turnover appears to capture the effect of temperature. Our semi-mechanistic model suggests that spatial variation in traits can potentially be used to estimate spatial variation in productivity at the landscape scale.

**Keywords**

Andes, climate, functional traits, global ecosystem monitoring, modelling, TFS, tropical forests.

*Ecology Letters* (2017)

## INTRODUCTION

One of the major challenges in contemporary ecosystem science is to understand how ecosystems respond to changes in environmental conditions, and how taxonomic and functional diversity mediate these changes (Lavorel & Garnier 2002). Environmental conditions change both in time and in space, and transects along environmental gradients can provide valuable insights into controls of ecosystem function. Tropical forest environmental gradients present a particularly rich study system (Vazquez & Givnish 1998; Wright 2002), with their high diversity facilitating general insights into the relationships between diversity and function that are not contingent on the characteristics and the presence or absence of particular dominant species. More specifically, tropical elevation gradients, with their usually high levels of soil moisture and year-long growing season, provide 'natural laboratories' to understand the influence of temperature on ecosystem

function without the complicating influence of variation in temperature seasonality and winter dormant seasons (Malhi *et al.* 2010; Sundqvist *et al.* 2013).

It is valuable to distinguish direct environmental controls on ecosystem productivity from indirect controls mediated through forest structure and composition, and to determine the degree to which productivity can be estimated from surveying ecosystem composition. Environmental conditions are usually considered direct drivers of ecosystem productivity (Fig. 1). Although in most tropical regions temperature is not a limiting factor on productivity, some studies suggest that across sites, tree growth increases with mean temperature (Raich *et al.* 1997; Cleveland *et al.* 2011) within the temperature range of currently observed tropical climates. In seasonal tropical forests, rainfall is positively associated with tree growth (Brienen & Zuidema 2005), while other studies identify solar radiation as a key driver of forest productivity across Amazonia (Nemani *et al.* 2003) particularly during the rainy season (Graham *et al.* 2003). Soil

[1]*Environmental Change Institute, School of Geography and the Environment, University of Oxford, Oxford, UK*
[2]*Department of Global Ecology, Carnegie Institution for Science, 260 Panama Street, Stanford, CA 94305, USA*
[3]*ARC Centre of Excellence in Plant Energy Biology, Research School of Biology, The Australian National University, Building 134, Canberra, ACT 2601, Australia*
[4]*Instituto Multidisciplinario de Biología Vegetal (IMBIV), CONICET and FCEFyN, Universidad Nacional de Córdoba, Casilla de Correo 495, Córdoba 5000, Argentina*
[5]*Department of Ecology and Evolutionary Biology, University of Arizona, Tucson, AZ 85721, USA*
[6]*The Santa Fe Institute, 1399 Hyde Park Rd, Santa Fe, New Mexico 87501, USA*
[7]*Department of Biology, Wake Forest University, Winston Salem, NC, USA*
[8]*Ecology and Global Change, School of Geography, University of Leeds, Leeds, UK*

[9]*Centre for Ecological Research and Forestry Applications (CREAF), Universidad Autonoma de Barcelona, Edificio C, 08290 Cerdanyola, Barcelona Spain*
[10]*School of Geosciences, University of Edinburgh, EH9 3FF, Edinburgh, UK*
[11]*Universidad Nacional de San Antonio Abad del Cusco, 733 Avenida de la Cultura, Cusco 921, Peru*
[12]*Centre for Tropical Environmental and Sustainability Science, College of Marine and Environmental Sciences, James Cook University, Cairns Qld, Australia*
[13]*Division of Plant Sciences, Research School of Biology, The Australian National University, Building 134, Canberra ACT 2601, Australia*
[14]*Sección Química, Pontificia Universidad Católica del Perú, San Miguel, Lima, Peru*
[15]*Faculty of Agriculture, University of Peradeniya, Peradeniya 20400, Sri Lanka*
[16]*Department Geography, College of Life and Environmental Sciences, University of Exeter, Amory Building EX4 4RJ, Exeter, UK*
*Correspondence: E-mail: nfyllas@gmail.com*

fertility may be important: in lowland tropical forest, phosphorus (P) availability is considered a key limiting factor of primary productivity (Quesada *et al.* 2012), whereas in montane regions with colder and younger soils, nitrogen (N) may be the limiting factor (Tanner *et al.* 1998). In summary, increases in one of the above factors can have positive effect on tree growth (given no other resource limitation), expressing a direct ('proximal') and short-term effect of environmental conditions on ecosystem productivity (Fig. 1).

Environmental conditions can additionally have an indirect ('distal') effect on forest productivity by regulating the structure and/or the species/functional composition of the community (Fig. 1). Such effects tend to act on longer temporal scales, where potential feedbacks between structure and functional composition can also take place. Many studies have shown that functional traits systematically vary with water availability (Santiago *et al.* 2004), soil fertility (Fyllas *et al.* 2009) and stand development (Lebrija-Trejos *et al.* 2010), and trait variation can predict individual-tree growth rate (Poorter *et al.* 2008) and community productivity (Finegan *et al.* 2015). However, feedbacks among environmental conditions, stand structure and functional composition have also been identified. For example, across Amazonia there exists a structural feedback on productivity, with rich soils favouring low biomass, fast-growing species in contrast to poor soils that favour high biomass slow-growing species (Baraloto *et al.* 2011; Quesada *et al.* 2012).

Disentangling the role of environmental and biotic controls on tropical forest productivity requires appropriate data sets.
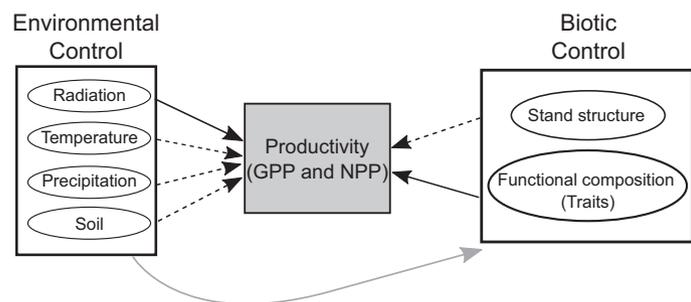


**Figure 1** Environmental and biotic controls on primary productivity. Environmental factors, such as radiation, temperature and precipitation, can have direct effects (black arrows) on GPP and net primary productivity (NPP) and/or indirect effects (grey arrow) through the regulation of stand structure and functional composition (expressed here as the distribution of functional traits). Biotic controls related to the stand structure and its functional composition can also have direct effect on primary productivity (black arrows). However, stand structure and functional composition are not only regulated by environmental factors as, for example, the biogeographic and disturbance history of the region, could also play a significant role. In this study, we explore the roles of a number of environmental and biotic controls (dashed and solid black arrows) and find that only two factors (traits and radiation; solid black lines) are required to explain the elevational trend in productivity. This study does not address how environmental factors influence biotic attributes (grey arrow). Stand structure is defined in this study as the number of trees and their diameter distribution within a plot. Functional composition is defined by the distribution of four functional traits ($LMA$, $N_L$, $P_L$ and $\rho_W$). Field-based estimates of GPP and NPP are made from inventory data and autotrophic respiration measurements. A trait-spectra individual-based model is used to simulate GPP and NPP by upscaling tree diameter and functional traits measurements.

In recent years, a large body of data has been emerging from an elevation transect in the Andes and Amazon in SE Peru, including rates of ecosystem carbon cycling (Girardin *et al.* 2010; Malhi *et al.* 2017a), forest structure and dynamics (Feeley *et al.* 2011; Asner *et al.* 2014a), plant ecophysiology (van de Weg *et al.* 2009, 2012; Bahar *et al.* 2016), and leaf and wood traits (Asner *et al.* 2014b; Malhi *et al.* 2017b). Along this 3300 m gradient, there is a steep temperature decrease with increasing elevation, a reduction in solar radiation and an increase in soil N and P content that drive high species turnover (Malhi *et al.* 2017a). This species turnover is associated with shifts in several functional traits including increasing leaf mass per area ($LMA$) and leaf P concentration with elevation (Asner *et al.* 2014b). Forest stature and structure vary greatly between lowland and highland plots, resulting in a decline in biomass with elevation and more open forests in the mountains (Asner *et al.* 2014a; Malhi *et al.* 2017a). Productivity declines with elevation but with some evidence of a step-change decline near the cloud base (Malhi *et al.* 2017a). It thus seems that various direct and indirect factors can potentially control forest productivity along the Andes-Amazon gradient. The available data sets present a unique opportunity to mechanistically explore the influence of climate, plant functional traits and forest structure on forest productivity.

Individual-based vegetation models provide an ideal framework to integrate forest inventory data with ecosystem dynamics theory and to explore how climate, functional traits and stand structure control primary productivity (Purves & Pacala 2008). In particular, by accounting for interspecific functional variation as well as tree-size variation, the performance of alternative life history strategies can be explored (Moorcroft *et al.* 2001; Scheiter *et al.* 2013). Functional traits are extensively used as predictors of plant processes. For example, $LMA$ and mass-based leaf nitrogen ($N_{Lm}$) and phosphorus ($P_{Lm}$) concentration are the central elements of the leaf economic spectrum and can be used to predict mass-based photosynthetic and respiration rates (Wright *et al.* 2004; Atkin *et al.* 2015), while wood density ($\rho_W$) and maximum height ($H_{max}$) appear to be good predictors of tree growth and mortality rates (Poorter *et al.* 2008; Wright *et al.* 2010).

In this study, we use a simplified version of a trait-spectra and individual-based model of tropical forest dynamics (TFS, Fyllas *et al.* 2014) to disentangle the relative importance of climate (direct environmental effect), stand structure and functional traits (indirect environmental effects) in controlling forest productivity along the Andes-Amazon elevation gradient. We initially apply the model along the gradient and validate its performance against field-based estimates of productivity. We subsequently exploit the model framework to perform a set of randomisation exercises designed to quantify the relative importance of climate, stand structure and functional traits in determining the observed patterns of forest productivity.

## MATERIALS AND METHODS

### Study site

The study area is located along a 3300 m elevation gradient in the tropical Andes and extends to the Amazon Basin.

Across this transect, a group of nine intensively monitored 1-ha plots (Table S1.1) was established as part of the long-term research effort coordinated by the Andes Biodiversity Ecosystems Research Group (ABERG, http://www.andesconservation.org) and the ForestPlots (https://www.forestplots.net/) and Global Ecosystems Monitoring Network (GEM; http://gem.tropicalforests.ox.ac.uk/projects/aberg) networks. Five of the plots are montane plots in the Kosñipata Valley, spanning an elevation range 1500–3500 m (Malhi *et al.* 2010), two are submontane plots located in the Pantiacolla front range of the Andes (600–900 m) and two plots are found in the Amazon lowlands in Tambopata National Park (200–225 m). The elevation gradient is very moist (Table S1.1), with seasonal cloud immersion common above 1500 m elevation (Halladay *et al.* 2012), and no clear evidence of seasonal or other soil moisture constraints throughout the transect (Zimmermann *et al.* 2010). Plots were established between 2003 and 2013 in areas that have relatively homogeneous soil substrates and stand structure, as well as minimal evidence of human disturbance (Girardin *et al.* 2010).

### Field-based forest productivity estimates

At all plots, the GEM protocol for carbon cycle measurements was applied (Malhi *et al.* (2017a), see also Data S1). The field measurements estimated gross primary productivity (GPP, the total rate of carbon capture and storage) and net primary productivity (NPP the rate of carbon uptake after subtracting autotrophic respiration, here measured as the rate of biomass production of wood, canopy and fine roots). Within our study plots, all trees with a $D > 10$ cm were identified at the species level, and in selected subplots all trees with $D > 2$ cm were measured and identified. The GEM protocol involves measuring and summing all major components of NPP and autotrophic respiration monthly or seasonally (Malhi *et al.* 2017a). NPP estimation is based on: canopy litterfall, leaf loss to herbivory, aboveground woody productivity of medium-large ($D > 10$ cm) trees (every 3 months), annual census of wood productivity of small trees ($D$ 2–10 cm), branch turnover on live trees, fine root productivity from ingrowth cores installed and harvested (every 3 months), and estimation of coarse root productivity from aboveground productivity. Autotrophic respiration ($R_a$) is calculated by summing up rhizosphere respiration (measured monthly), aboveground woody respiration estimated from stem respiration measurements (monthly) and scaling with surface area, belowground coarse root and bole respiration (fixed multiplier to stem respiration) and leaf dark respiration estimated from measurements of multiple leaves in two seasons. GPP is estimated from the amount of carbon used for NPP and $R_a$, thus GPP = NPP + $R_a$. Carbon use efficiency is given by $c$ = NPP/GPP. We note that only a relatively small component of GPP and NPP (woody NPP) is based on diameter at breast height ($D$) measurements, with larger components coming from litterfall and respiration and fine root turnover. Wood productivity accounts for only around 10% of GPP and 25% of NPP (Malhi *et al.* 2017a), and the relationship between wood production and total NPP or GPP is weak (Malhi *et al.* 2011). These estimates

are used as our best guess of stand-level GPP and NPP although we acknowledge that they involve a number of assumptions.

### Model description

The original TFS model is a trait-continua and individual-based model, which simulates the carbon (C) balance of each tree in a stand (Fyllas *et al.* 2014), taking into account light competition (Strigul *et al.* 2008). In the original model, the carbon balance of each tree is estimated using a coupled photosynthesis stomatal conductance model. The parameters of the photosynthetic model are estimated from three leaf functional traits ($LMA$, $N_{Lm}$ and $P_{Lm}$) that regulate the photosynthetic capacity and the respiration rate of trees. Rather than grouping trees into plant functional types, TFS prescribes interrelated joint distributions of functional traits which represent trade-offs of possible plant strategies and responses to environmental conditions. In addition to the leaf traits, wood density ($\rho_W$) is used to account for variation in aboveground biomass ($M_A$) and mortality rates.

Here, we use a simplified version of TFS (described in Data S2), where the mechanistic representation of photosynthesis, respiration and C allocation is replaced by a simple tree-growth equation, where a time-integrated whole-tree averaged photosynthetic rate is multiplied by the total leaf area of a tree to estimate total biomass increment (Lambers *et al.* 1989; Walters & Reich 1999; Enquist *et al.* 2007):

$$\frac{dM_T}{dt} = \left(\frac{c}{\omega}A_L\right)\left(\frac{1}{LMA}\right)M_L \tag{1}$$

with $M_T$ the total plant dry biomass (kg), $c$ the carbon use efficiency (no units), $\omega$ the fraction of whole-plant dry mass that is carbon, $\dot{A}_L$ the leaf area specific photosynthetic rate (g C cm$^{-2}$ per unit time), $LMA$ leaf dry mass per area (kg m$^{-2}$) and $M_L$ the total leaf dry mass (kg). The growth of each tree is estimated on a daily time-step. Annual tree growth (NPP) is given by summing all daily $dM_T$. Annual GPP is estimated by dividing d$M_T$ by $c$ and summing all daily values. All simulations are performed in a snapshot mode, i.e. for 1 year where $M_L$ is constant.

Allometric equations, with varying scaling coefficients estimated from available data, are used to allocate plant biomass to different plant components including leaf biomass. In addition, the photosynthetic rate of each tree is expressed as a function of both leaf traits (that vary in a continuous way across individuals) and irradiance that takes into account competition for light between individuals. In the following paragraphs, we describe how the model was parameterised with available field and literature data. The main model parameters are summarised in Table 1, and a sensitivity analysis of simulated GPP for some of the key model parameters is provided in Data S2.

### Model initialisation

Within our study plots, all trees with a $D > 10$ cm have been identified at the species level. In addition $LMA$, $N_{Lm}$, $P_{Lm}$ and $\rho_W$ were measured (Asner *et al.* 2016b; Malhi *et al.* 2017b) for

**Table 1** Key model parameters of the simplified tropical forest dynamics (TFS) model used in this study

| Parameter | Description | Input/equation | Origin |
|---|---|---|---|
| $D$ | Diameter at breast height | Inventory data | Malhi *et al.* (2017a) |
| $LMA$ | Leaf dry mass per area | Inventory data | Malhi *et al.* (2017a) |
| $N_L$ | Leaf $N$ content | Inventory data | Malhi *et al.* (2017a) |
| $P_L$ | Leaf $P$ content | Inventory data | Malhi *et al.* (2017a) |
| $\rho_W$ | Wood density | Inventory data | Malhi *et al.* (2017a) |
| $H$ | Tree height | $H = \exp(\alpha_H + \beta_H D)$ | Shenkin *et al.* (2017) |
| $C_A$ | Crown area | $C_A = \alpha_c D^{\beta_c}$ | Shenkin *et al.* (2017) |
| $M_A$ | Aboveground biomass | $M_A = \alpha_A \cdot (\rho_w \cdot D^2 \cdot H)^{\beta_A}$ | Chave *et al.* (2014) |
| $M_L$ | Leaf biomass | $M_L = \alpha_L \cdot M_A^{\beta_L}$ | This study |
| $\dot{A}_L$ | Leaf photosynthetic rate | $\dot{A}_L = (A_{\max} \cdot I/(k+I)) - R_d$ | This study |
| $I$ | Irradiance | $I = a \cdot I \cdot \exp(-0.5 \cdot SLAI)$ | Modelled |
| $a$ | Leaf absorptance | $a = 0.75$ | Assumed |
| SLAI | Shading leaf area index | Modelled | Modelled |
| $A_{\max}$ | Max photosynthetic rate | $A_{\max} = 10.25$ or $A_{\max} = f(P_L)$ | Table S2.1 |
| $k$ | Half saturation coefficient | $k = f(LMA, N_L, P_L)$ | Table S2.1 |
| $R_d$ | Respiration in the light | $R_d = f(LMA, N_L, P_L)$ | Table S2.1 |
| $c$ | Carbon use efficiency | $c = N(0.33, 0.04)$ | Malhi *et al.* (2017a) |
| $\omega$ | Carbon dry mass fraction | $\omega = 0.5$ | Assumed |
| $g(T)$ | Temperature response | $\max(0, -0.242 + 0.0937T - 0.00177T^2)$ | Higgins *et al.* (2016) |

Please see Data S2 for a complete model description.

approximately 7% of the stems of species that comprise 60% (in diverse lowland sites) to 80% (in the less diverse montane sites) of the total plot basal area. In our simulations, individuals with measured trait values were included as such, without using an average species value, in order to incorporate intraspecific variation. For the rest of the trees, trait values were populated hierarchically using, in the decreasing order of preference, the species mean plot value, the species transect-wide mean value or, for trees for which no species-level traits were available, the plot-level trait means.

Climate data were available from weather stations located close to each study site (Table S1.1). The most complete time series for most weather stations were for the year 2013 and solar radiation, temperature and precipitation were recorded at 30-min intervals. We used these time series to estimate average daily climate.

*Tree allometry*
Transect-wide allometric equations of tree height ($H$) and crown area ($C_A$) as a function of tree diameter were used to define the architecture of each tree in a stand (Shenkin *et al.* 2017). In the model, trees were considered to have a flat-topped circular canopy with an area equal to the allometrically estimated projected crown area.

Aboveground tree biomass ($M_A$ in kg) is estimated from the Chave *et al.* (2014) equation that takes into account the diameter, the wood density and the height of a tree. Total leaf biomass was expressed as a power function of $M_A$, parameterised using the BAAD dataset (Falster *et al.* 2015). During simulations, we allowed the coefficients of the power functions to vary within their 95% confidence interval estimates, with individual trees having different leaf allometries (Table S2–Tree Allometry).

*Functional traits and photosynthesis*
The photosynthetic rate ($\dot{A}_L$) is controlled by the leaf functional traits and the available light of each individual. A

Michaelis–Menten (MM) model was used for that purpose where:

$$\dot{A}_L = \frac{A_{\max} I}{k + I} - R_d \qquad (2)$$

with $I$ (µmol m$^{-2}$s$^{-1}$) the irradiance at the top of each individual, $A_{\max}$ the maximum gross photosynthetic rate (µmol m$^{-2}$s$^{-1}$), $k$ the half saturation coefficient (µmol m$^{-2}$s$^{-1}$) and $R_d$ is the non-photorespiratory mitochondrial $CO_2$ release taking place in the light (i.e. respiration in the light) (µmol m$^{-2}$s$^{-1}$).

The irradiance $I$ is estimated through the light competition scheme, while the three leaf functional traits ($LMA$, $N_L$ and $P_L$) regulate the parameters of the light response curve (Marino *et al.* 2010). An independent data set of 136 light response curves and $LMA$, $N_L$ and $P_L$ measurements (Atkin *et al.* 2015) was available for 14 study sites along the Andean elevation gradient. These data were used to fit MM light response curves and express their parameters ($A_{\max}$, $k$ and $R_d$) as a function of the leaf functional traits (Data S2-Photosynthesis). An average daily $\dot{A}_L$ is estimated using equation 2 and average daily irradiance, with the total daily $A_L$ given after multiplying average $\dot{A}_L$ with the day length.

Analyses in Bahar *et al.* (2016) and here (Data S2-Photosynthesis) suggest that across the Andean gradient the maximum light-saturated photosynthetic rate does not vary with elevation. Thus, photosynthesis strongly acclimates to prevailing air temperature and this supports the use of a temperature-independent model of leaf photosynthesis in our simulations. However, in order to specifically test for the importance of direct temperature effects on photosynthesis, we used a generic temperature sensitivity model (Higgins *et al.* 2016) and compared simulations with and without temperature dependence.

**Simulations**

We performed two sets of simulations to elucidate the major controls of forest productivity along the Amazon-Andes

gradient. First, the importance of temperature sensitivity was explored following a 'leave-one-out' procedure that explored the ability of TFS to simulate GPP and NPP patterns under four different model setups that accounted for: (1) photosynthetic temperature sensitivity (PTS), variation in functional traits along the gradient (FTV) and the effects of traits on $A_{max}$ (P$-A_{max}$), (2) PTS + FTV, (3) only PTS and (4) only FTV. The P$-A_{max}$ parameterisation accounts for the positive effect of $P_L$ on $A_{max}$ and it was used to explore for potential counteracting effects of temperature and $P_L$ on photosynthetic rate that could cancel each other out if considered separately.

Secondly, to explore the importance of climate, stand structure and functional traits in determining GPP and NPP across our study sites, we applied within TFS a set of randomisation exercises. These are described in detail in Data S3. To test the importance of climate (*Climate only Setup – CoS*), we simulated GPP and NPP using the local (plot-specific) climate and a regional average stand structure and trait distribution (i.e. the average stand structure and traits distribution across all plots along the transect). The hypothesis behind *CoS* is that climate, and particularly variation in incoming solar radiation, is sufficient to explain variation in productivity across the elevation gradient, with no between-plots variation in traits or stand structure required. The role of stand structure was tested using the *Structure only Setup (SoS)*. Following this setup, the observed $D$ distribution in each plot was used to initialise trees, while climate and functional diversity were

kept constant. The hypothesis behind the *SoS* is that change in stand structure, via its effects on the partitioning of available light, is the most important determinant of productivity along the elevation gradient. Finally, the potential control of functional trait variation, expressed through the distributions of the four traits, was explored by initialising TFS with the locally measured trait distribution while keeping climate and stand-size distribution fixed [*Traits only Setup (ToS)*]. The hypothesis tested by this setup is that knowledge of the local distribution of the four functional traits is adequate to predict observed variation in GPP and NPP with elevation.

## RESULTS

The predictive ability of the various model setups were quantified through standardised major axis (SMA) regressions and estimation of root mean square error (RMSE in MgC ha$^{-1}$ year$^{-1}$) between field estimated (observed) and simulated GPP and NPP. In addition, ordinary least square regressions of simulated GPP and NPP with elevation were performed with the estimated slope ($\beta_{OLS}$ in MgC ha$^{-1}$ year$^{-1}$ km$^{-1}$) representing the sensitivity of each setup to changes in elevation.

All simulations that included photosynthetic temperature dependence were over-sensitive to elevation changes, underestimating both GPP and NPP particularly at upland sites (Fig. 2, Table S5.1). Even when the positive $A_{max}$-$P_{La}$ effect was
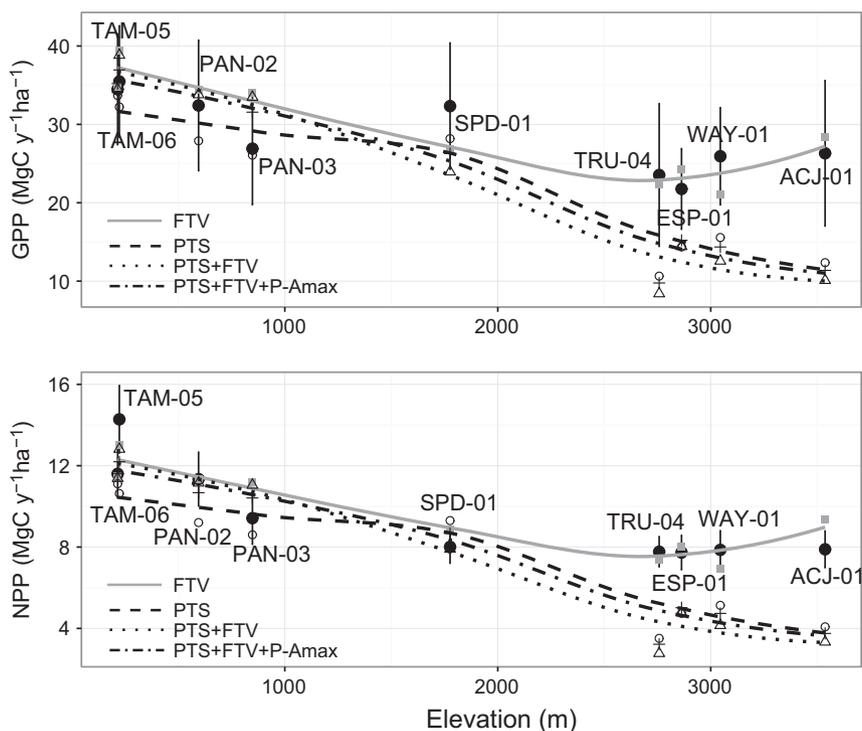


**Figure 2** Observed (field estimated) and simulated GPP (upper panel) and net primary productivity (NPP) (lower panel) along the Andes-Amazon transect. Black circles are observations (± 2 standard error). Grey squares and line show simulations with no temperature dependence of photosynthesis but with functional traits variation (FTV) along the elevation gradient. Open circles indicate simulations including temperature sensitivity but no functional traits shift along the gradient [photosynthetic temperature sensitivity (PTS)]. Triangles indicate simulations accounting for temperature dependence of photosynthesis and functional traits shift along the gradient (PTS+FTV). Crosses show simulations with photosynthetic temperature dependence, functional trait variation and a positive effect of leaf P content on $A_{max}$ (PTS+FTV+P-$A_{max}$). Lines present local polynomial regressions (loess) of simulated GPP and NPP with elevation under the different model setups.

enabled, productivity was underestimated at upland sites suggesting that the relative effect of $P_{La}$ is lower than that of temperature. However, when trait values were allowed to vary with elevation in accordance with observations and temperature sensitivity was excluded, the model performed best [GPP: RMSE = 3.87, $\beta_{OLS}$ = −4.24, NPP: RMSE = 0.99, $\beta_{OLS}$ = −1.40]. We named this model setup, initialised with plot-specific solar radiation, stand structure and functional traits data, as the fully constrained model setup (*FcS*). We note here that accounting for light competition was particularly important for accurate GPP and NPP simulations (Fig. S5.2, Table S5.2). The *FcS* captures the broad gradient between higher productivity in lowland sites and lower productivity in montane sites, suggesting that direct photosynthetic temperature sensitivity could be excluded from our modelling framework (although it could still matter through its effects on traits), and that across the gradient solar radiation is the main climatic driver of spatial variation in forest productivity.

After validating the model, we used the randomisation exercises to test the importance of climate, stand structure and functional traits to drive GPP and NPP patterns. When exploring for the effects of climate (*CoS*), i.e. factoring out stand structure and traits variation, the RMSE increased both for GPP and NPP [3.99 and 1.99, respectively] and the model was less sensitive to elevation changes [$\beta_{OLS}$ = −1.40 and $\beta_{OLS}$ = −0.46, respectively] (Table 2). Hence, *CoS* captured the mean productivity across the gradient but was not as sensitive as *FcS* to changes in elevation and in particular overestimated forest productivity at upland sites (Fig. 3).

When site-specific structure was used as the main driver (*SoS*), there was a substantial decline in the predictive ability of the model. The broad scale decline of primary productivity with elevation could not be reproduced adequately (Fig. 3), and RMSE increased both for GPP and NPP (Table 2). This suggests that knowledge of the tree-size distribution alone is not enough to estimate patterns of productivity along the

Andean elevation gradient. It should be remembered, however, that the *SoS* setup represents mainly variation in size-class distribution and not variation in established biomass, which in the model is additionally influenced by variation in wood density.

When functional trait variation alone was considered (*ToS*), the model reproduced the broad scale decline with elevation but both GPP and NPP were overestimated compared to *FcS*, particularly at mid-elevations (Fig. 3). For GPP, the RMSE increased [5.38] compared to the *FcS* and the *CoS* but the sensitivity of the model to elevation was close to observations [$\beta_{OLS}$ = −3.26] (Table 2). For NPP, the RMSE [1.64] was higher than *FcS* but lower than *CoS* and sensitivity with elevation [$\beta_{OLS}$ = −1.08] was higher than *CoS*. These results suggest that the local traits distributions captures the declining trend in productivity with elevation, but additional knowledge of solar radiation, is required to accurately estimate GPP and NPP.

To gain further insights into the mechanisms that drive variation in forest productivity, we explored how some key stand-level parameters vary with elevation using inferences from the *FcS* (Fig. 4). Average light availability over all canopy depths ($I_m$) declines with elevation and then increases at the uppermost plot, following variation in incoming solar radiation at the top of the canopy ($S_O$) and inversely the number of stems per area ($N_S$). On the other hand, the basal area-weighted average *LMA* and $P_{La}$ increase with elevation, while $N_{La}$ does not change much. Simulated $R_d$ does not vary much across the gradient and given the constant $A_{max}$ the decline in actual photosynthesis ($A_L$) is mainly a result of variation in light availability, with a small divergence at the uppermost plots. However, the half saturation coefficient also increases with elevation and this suggests that trees at upland sites have a lower photosynthetic rate for a given light intensity (below maximum rates) compared to their lowland counterparts, explaining the divergence in $\dot{A}_L$. Thus, reductions in average photosynthetic rate with elevation are likely to be mainly due

**Table 2** Results of tropical forest dynamics (TFS) performance under different setups

| Setup | ρ simulations-observations | Slope simulations-observations ($\beta_{SMA}$) | RMSE simulations-observations | Slope simulations-elevation ($\beta_{OLS}$) |
|---|---|---|---|---|
| **GPP** | | | | |
| ***FcS:*** Fully constrained | **0.77** | 1.03 (0.93–1.14) | 3.87 | −4.24 (± 0.90) |
| ***CoS:*** Local climate | **0.79** | 1.09 (1.00–1.18) | 3.99 | −1.40 (± 0.83) |
| ***SoS:*** Local stand structure | 0.06 | | 4.92 | 0.51 (± 0.41) |
| ***ToS:*** Local traits | 0.51 | | 5.38 | −3.26 (± 0.69) |
| **NPP** | | | | |
| ***FcS:*** Fully constrained | **0.90** | 1.01 (0.93–1.10) | 0.99 | −1.40 (± 0.30) |
| ***CoS:*** Local climate | **0.60** | 1.07 (0.92–1.24) | 1.99 | −0.46 (± 0.27) |
| ***SoS:*** Local stand structure | −0.31 | | 2.13 | 0.17 (± 0.13) |
| ***ToS:*** Local traits | **0.62** | 1.07 (0.93–1.24) | 1.64 | −1.08 (± 0.23) |

Bold values of the Pearson's correlation coefficient (ρ) between field measurements and simulations indicate a statistical significant associations ($P < 0.05$). In cases of significant correlations a SMA regression was fit and the slope $\beta_{SMA}$ along with a 95% CI is reported. An adequate model performance is considered when $\beta_{SMA}$ estimates include 1. RMSE (Mg C ha$^{-1}$ year$^{-1}$) between observations and simulations are also reported with lower values indicating a better model performance. The slope of an ordinary least square regression of simulated productivity with elevation $\beta_{OLS}$ (± standard error) is also reported here to summarise the sensitivity of GPP and NPP with elevation. For comparison the estimated slope from observations for GPP is −3.05 (Mg C ha$^{-1}$ year$^{-1}$ km$^{-1}$) and for NPP is −1.53 (Mg C ha$^{-1}$ year$^{-1}$ km$^{-1}$).
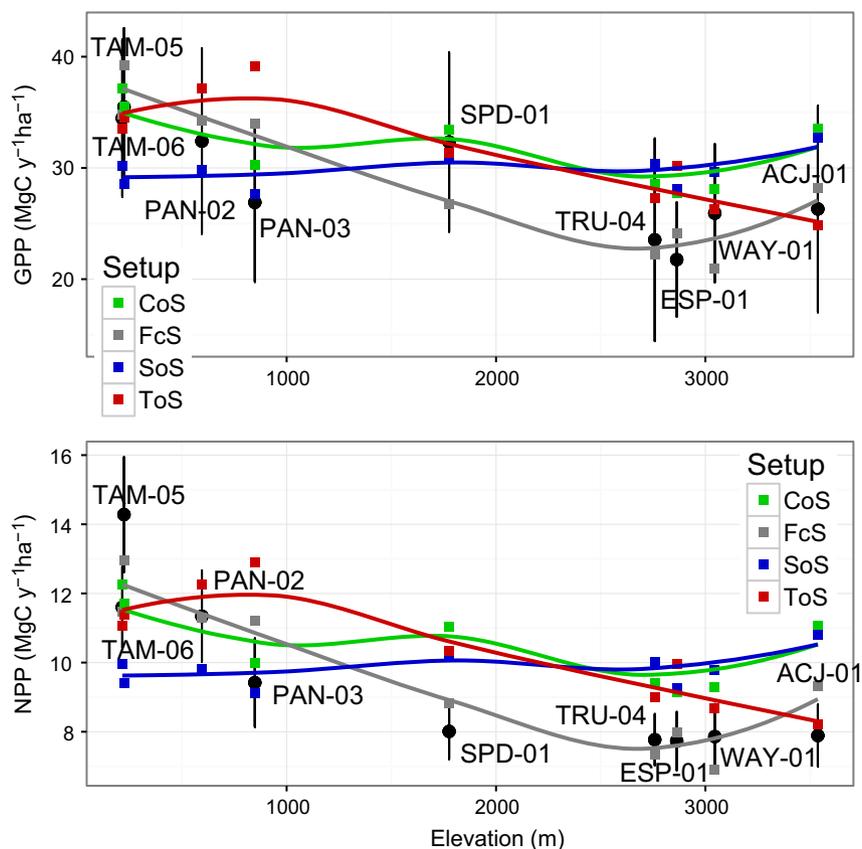
**Figure 3** Simulated GPP (upper panel) and net primary productivity (NPP) (lower panel) under the different model setups. Grey points indicate GPP or NPP simulations following the fully constrained model setup (*FcS*). Green points present simulations using the local climate (*CoS*) and average regional structure and trait data. Blue points present simulations using the local stand structure (*SoS*) and average regional climate and trait data. Red points present simulations using the local traits distributions (*ToS*) and regional climate and stand structure data. Black points indicate estimates of GPP or NPP from field measurements ± 2 standard errors. Line presents local polynomial regressions (loess) of simulated GPP or NPP with elevation for each model setup.

to reductions in light availability as well as due to the higher light levels required for photosynthetic light saturation for trees at higher elevations.

## DISCUSSION

Various environmental and biotic drivers can control forest productivity along the Amazon-Andes elevation gradient (Fig. 1). We developed a simplified version of a vegetation model that integrates a range of field measurements in order to understand the relative importance of climate, stand structure and functional traits on forest productivity. Overall, TFS provided simulations that were in line with field estimates of the magnitude and trends in GPP and NPP across the elevation gradient. In the following paragraphs, we describe how the performed simulations and randomisation exercises were used to understand the decline in productivity with elevation.

### Temperature and photosynthesis acclimation

Variation in primary productivity has been traditionally considered to reflect the effects of climate variables such as radiation, temperature and precipitation on plant metabolic rates (Chapin *et al*. 2011). A recent study reported that, along the Andean elevation gradient, maximum carboxylation and electron transport rates at a standardised temperature of 25 °C were significantly higher at upland sites, possibly reflecting greater *P* per unit leaf area at high elevations and/or thermal acclimation to sustained lower growth temperatures (Bahar *et al*. 2016). By contrast, when measurements of gas exchange were made at the daytime temperatures at each site (20–28 °C; Fig. S2.2), light-saturated, area-based rates of net photosynthesis, as well as maximum carboxylation and electron transport rates, show no significant trend with elevation (Bahar *et al*. 2016; Malhi *et al*. 2017a). The latter observations support the use of a temperature-independent equation for photosynthetic carbon assimilation. Our simulations show that accurate GPP and NPP predictions can be made without a direct temperature sensitivity effect on photosynthesis (Fig. 2). When both temperature sensitivity and functional traits variation was included in the model, forest productivity was too sensitive to elevation changes. This suggests that the effect of temperature is likely to be manifested through variation in leaf traits, which may be controlled by variation in environmental conditions (including temperature) along the gradient. The shift in leaf traits and photosynthetic characteristics with elevation cancels out much of the ecophysiological temperature dependency found in single plant measurements. This does not imply that short-term temperature changes (months to decades) will not affect forest productivity but rather that long-term changes lead to a turnover in species such
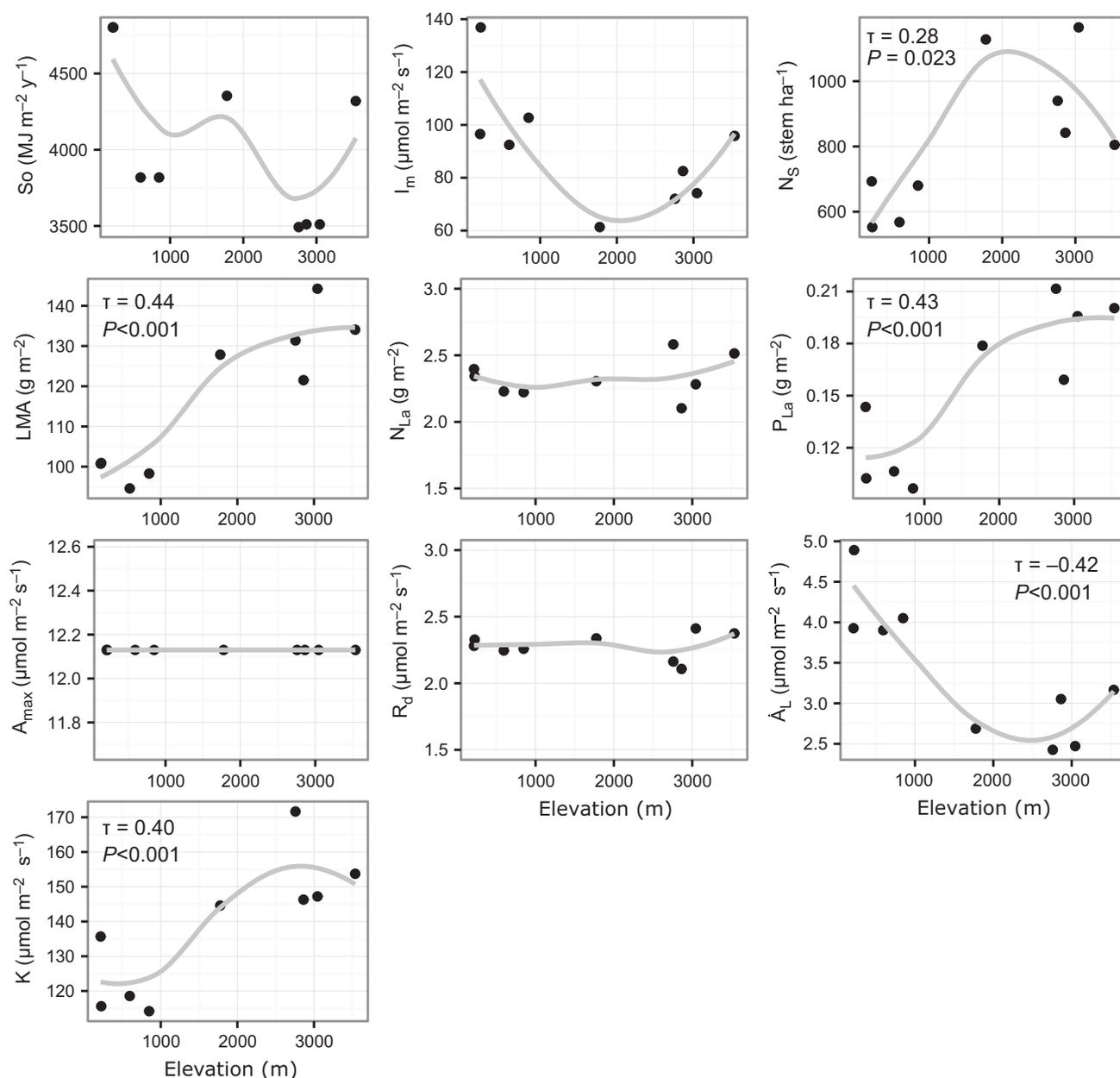
**Figure 4** Elevational variation of key stand-level parameters inferred from the fully constrained (*FcS*) model setup. $S_O$ (MJ m$^{-2}$ year$^{-1}$) is the total annual incoming solar radiation at the top of the canopy, $I_m$ (µmol m$^{-2}$ s$^{-1}$) is the average annual light availability across all canopy layers, $N_S$ (stems ha$^{-1}$) the number of stems per area, *LMA* (g m$^{-2}$) the basal area-weighted average leaf dry mass per area, $N_{La}$ and $P_{La}$ the average basal area-weighted N and P concentrations, $A_{max}$ (µmol m$^{-2}$ s$^{-1}$) the average maximum photosynthetic rate, $R_d$ (µmol m$^{-2}$ s$^{-1}$) the average basal area-weighted respiration rate, $\dot{A}_L$ (µmol m$^{-2}$ s$^{-1}$) average annual basal area-weighted actual photosynthetic rate and *K* (µmol m$^{-2}$ s$^{-1}$) average basal area-weighted half saturation coefficient. Kendall correlations coefficients (τ) are displayed for all stand-level parameters where a statistically significant association with elevation was identified.

that the local community is acclimated to local growing conditions, resulting in little sensitivity of productivity to temperature on long time scales, and within the temperature range studied. An alternative possibility is that temperature shows a strong but non-causal relationship with leaf traits along the gradient, and this obscures a real direct temperature effect.

**Functional traits**

Previous studies along this and other elevation gradients in the Andes region found that more than 80% of *LMA* and $N_L$

turnover between communities is determined phylogenetically, suggesting that these traits may have been involved in evolutionary adaptation (Asner *et al.* 2014b). Furthermore, Asner *et al.* (2014b) found that these intercommunity differences in *LMA* and $N_L$ were dominated by changes in temperature, rather than by other factors such as moisture or radiation. By contrast, between-community variation in $P_L$ is controlled by substrate rather than temperature effects (Asner *et al.* 2016b). Along the Amazon-Andes gradient leaf N:P ratio declines with elevation (Malhi *et al.* 2017b) and this might indicate a switch from P to N limited photosynthesis consistent with soil

properties (Nottingham *et al.* 2015), with Bahar *et al.* (2016) suggesting that knowledge of growth temperature is not required to estimate photosynthetic capacity if leaf and soil P data are available. Here, we used empirical relationships to infer the parameters of the photosynthetic light response curve form $LMA$, $N_{La}$ and $P_{La}$ and thus determine how changes in traits regulate C-fixation. In an additional simulation exercise, the progressive increase in the functional strategies included in the model (from one Plant Functional Type (PFT), to nine PFTs, to a continuum of plant strategies), increased the predictive ability of the model. This outcome suggests that species turnover (Malhi *et al.* 2017a) and the associated shifts in plant functional traits is a stronger driver of spatial variation in forest productivity than direct environmental filtering effects (S5–Importance of elevation shifts in functional traits).

### Solar radiation and light competition

Along the Andean gradient, solar radiation declines at mid-high elevations, associated with a higher frequency of both cloud occurrence and cloud immersion (Halladay *et al.* 2012), and then rises again at the uppermost treeline plot. In our simulations, the actual photosynthetic rate follows variation in light availability, while at the uppermost plots this relationship could be additionally controlled by the higher photosynthetic light saturation level that characterises upland trees (Fig. 4). Thus, solar radiation is the strongest direct climatic determinant of forest productivity, and therefore, actual photosynthesis does not track potential photosynthesis (van de Weg *et al.* 2014; Malhi *et al.* 2017a). One of the key criticisms of classical Metabolic Scaling Theory is that it fails to account for asymmetric competition for light (Coomes & Allen 2009). The proposed modelling framework addresses this issue by explicitly simulating the hierarchical position of each individual within a stand, using the perfect-plasticity approximation assumption (Strigul *et al.* 2008). Our simulations show that inclusion of light competition is necessary for accurately predicting GPP and NPP (S5–Light Competition).

### Stand structure

Our simulations suggest that stand structure and in particular diameter distribution do not have a strong effect on forests productivity along our study plots. Although woody biomass declines with elevation, basal area does not (Malhi *et al.* 2017b). This constancy of basal area may diminish the effect of biomass variation in contrast with studies that identify biomass as the strongest predictor of forest productivity, for example during succession (Lohbeck *et al.* 2015). Thus, in mature stands, like the ones studied here, variation in functional traits that control carbon assimilation and biomass allocation might be stronger predictors of forest productivity than standing biomass (Finegan *et al.* 2015). In our case, this functional trait variation seems to be primarily controlled by species turnover.

### CONCLUSIONS

Here, we combine a uniquely rich data set of plot-level productivity coupled with functional traits and a modelling framework to understand what drives the trend of productivity along a tropical forest elevation gradient. We have shown that an individual-based model that explicitly describes functional trait variation within and between plots, and accounts for light competition can realistically capture variation in primary productivity along the investigated gradient. Our findings suggest that the decline in productivity with increasing elevation is explained by a combination of shifts in plant traits values and a decline in solar radiation. Remarkably, we do not need to account for direct temperature dependence of photosynthesis, beyond what may be an effect of temperature through the observed plant traits. The turnover in the plant community and ensuing shift in plant traits cancels much of the temperature dependency that is found in single plant *in situ* measurements. The work not only demonstrates the utility of tropical elevation transects in yielding important insights into long-term ecosystem sensitivity to temperature, but also suggests that variation in solar radiation introduces a moderate complicating caveat. Advanced new techniques, such as airborne spectroscopy, have demonstrated the potential to map key leaf traits at landscape and regional scale, both along elevation gradients and across edaphic contrasts in the lowlands (Asner *et al.* 2014a, 2016a). Our work shows that this spatial variation in traits can translate into potentially mapping spatial variation in productivity at landscape scale, with spatial variation in leaf traits capturing much of the spatial variation in environmental conditions. However, mapping traits alone is not sufficient, and there is still a need to account for (i) variation in the abundance or dominance of traits not only in the canopy but also in the understory as well as (ii) light-limitation of photosynthesis. In combination with airborne mapping of canopy traits at large scale, this work opens the door to a mechanistic approach to mapping ecosystem productivity at landscape and regional scales.

## AUTHOR CONTRIBUTION

NMF and YM designed the research. LPB, AS, GPA, OKA, SD, BE, WF-R, RG, WHH, YI, REM, PM, NS, MS, KWLKW and JZ-C gathered the stand and functional traits data. NMF, LPB and AS analysed the field data. NMF developed the model and analysed simulations. NMF, LPB and YM wrote the manuscript with contributions from all authors.

## REFERENCES

Asner, G.P., Anderson, C.B., Martin, R.E., Knapp, D.E., Tupayachi, R., Sinca, F. *et al.* (2014a). Landscape-scale changes in forest structure and functional traits along an Andes-to-Amazon elevation gradient. *Biogeosciences*, 11, 843–856.

Asner, G.P., Martin, R.E., Tupayachi, R., Anderson, C.B., Sinca, F., Carranza-Jiménez, L. *et al.* (2014b). Amazonian functional diversity from forest canopy chemical assembly. *PNAS*, 111, 5604–5609.

Asner, G.P., Knapp, D.E., Anderson, C.B., Martin, R.E. & Vaughn, N. (2016a). Large-scale climatic and geophysical controls on the leaf economics spectrum. *PNAS*, 113, E4043–E4051.

Asner, G.P., Martin, R.E., Anderson, C.B., Kryston, K., Vaughn, N., Knapp, D.E. *et al.* (2016b). Scale dependence of canopy trait distributions along a tropical forest elevation gradient. *New Phytol.*, doi:10.1111/nph.14068, in press.

Atkin, O.K., Bloomfield, K.J., Reich, P.B., Tjoelker, M.G., Asner, G.P., Bonal, D. *et al.* (2015). Global variability in leaf respiration in relation to climate, plant functional types and leaf traits. *New Phytol.*, 206, 614–636.

Bahar, N.H.A., Ishida, F.Y., Weerasinghe, L.K., Guerrieri, R., O'Sullivan, O.S., Bloomfield, K.J. *et al.* (2016). Leaf-level photosynthetic capacity in lowland Amazonian and high-elevation Andean tropical moist forests of Peru. *New Phytol.*, doi:10.1111/nph.14079, in press.

Baraloto, C., Rabaud, S., Molto, Q., Blanc, L., Fortunel, C., Hérault, B. *et al.* (2011). Disentangling stand and environmental correlates of aboveground biomass in Amazonian forests. *Glob. Change Biol.*, 17, 2677–2688.

Brienen, R.J.W. & Zuidema, P.A. (2005). Relating tree growth to rainfall in Bolivian rain forests: a test for six species using tree ring analysis. *Oecologia*, 146, 1.

Chapin, F.S., Matson, P.A. & Vitousek, P.M. (2011). *Principles of terrestrial ecosystem ecology*. Springer New York, New York, NY.

Chave, J., Réjou-Méchain, M., Búrquez, A., Chidumayo, E., Colgan, M.S., Delitti, W.B. *et al.* (2014). Improved allometric models to estimate the aboveground biomass of tropical trees. *Glob. Change Biol.*, 20, 3177–3190.

Cleveland, C.C., Townsend, A.R., Taylor, P., Alvarez-Clare, S., Bustamante, M.M.C., Chuyong, G. *et al.* (2011). Relationships among net primary productivity, nutrients and climate in tropical rain forest: a pan-tropical analysis. *Ecol. Lett.*, 14, 939–947.

Coomes, D.A. & Allen, R.B. (2009). Testing the metabolic scaling theory of tree growth. *J. Ecol.*, 97, 1369–1373.

Enquist, B.J., Kerkhoff, A.J., Stark, S.C., Swenson, N.G., McCarthy, M.C. & Price, C.A. (2007). A general integrative model for scaling plant growth, carbon flux, and functional trait spectra. *Nature*, 449, 218–222.

Falster, D.S., Duursma, R.A., Ishihara, M.I., Barneche, D.R., FitzJohn, R.G., Vårhammar, A. *et al.* (2015). BAAD: a biomass and allometry database for woody plants. *Ecology*, 96, 1445.

Feeley, K.J., Silman, M.R., Bush, M.B., Farfan, W., Cabrera, K.G., Malhi, Y. *et al.* (2011). Upslope migration of Andean trees. *J. Biogeogr.*, 38, 783–791.

Finegan, B., Peña-Claros, M., de Oliveira, A., Ascarrunz, N., Bret-Harte, M.S., Carreño-Rocabado, G. *et al.* (2015). Does functional trait diversity predict above-ground biomass and productivity of tropical forests? Testing three alternative hypotheses. *J. Ecol.*, 103, 191–201.

Fyllas, N.M., Patiño, S., Baker, T.R., Bielefeld Nardoto, G., Martinelli, L.A., Quesada, C.A. *et al.* (2009). Basin-wide variations in foliar properties of Amazonian forest: phylogeny, soils and climate. *Biogeosciences*, 6, 2677–2708.

Fyllas, N.M., Gloor, E., Mercado, L.M., Sitch, S., Quesada, C.A., Domingues, T.F. *et al.* (2014). Analysing Amazonian forest productivity using a new individual and trait-based model (TFS v. 1). *Geosci. Model Dev.*, 7, 1251–1269.

Girardin, C.A.J., Malhi, Y., Aragão, L.E.O.C., Mamani, M., Huaraca Huasco, W., Durand, L. *et al.* (2010). Net primary productivity allocation and cycling of carbon along a tropical forest elevational transect in the Peruvian Andes. *Glob. Change Biol.*, 16, 3176–3192

Graham, E.A., Mulkey, S.S., Kitajima, K., Phillips, N.G. & Wright, S.J. (2003). Cloud cover limits net $CO_2$ uptake and growth of a rainforest tree during tropical rainy seasons. *PNAS*, 100, 572–576.

Halladay, K., Malhi, Y. & New, M. (2012). Cloud frequency climatology at the Andes/Amazon transition: 1. Seasonal and diurnal cycles. *J. Geophys. Res.*, 117, D23102.

Higgins, S.I., Buitenwerf, R. & Moncrieff, G.R. (2016). Defining functional biomes and monitoring their change globally. *Glob. Change Biol.*, 22, 3583–3593.

Lambers, H., Freijsen, N., Poorter, H., Hirose, T. & dervan Werff, H. (1989). Analyses of growth based on net assimilation rate and nitrogen productivity: their physiological back-ground. In: *Variation in Growth Rate and Productivity of Higher Plants* (eds Lambers, H., Cambridge, M.L., Konings, H. & Pons, T.L.). The Hague: SPB Academic Publishing, pp. 1

Lavorel, S. & Garnier, E. (2002). Predicting changes in community composition and ecosystem functioning from plant traits: revisiting the Holy Grail. *Funct. Ecol.*, 16, 545–556.

Lebrija-Trejos, E., Pérez-García, E.A., Meave, J.A., Bongers, F. & Poorter, L. (2010). Functional traits and environmental filtering drive community assembly in a species-rich tropical system. *Ecology*, 91, 386–398.

Lohbeck, M., Poorter, L., Martínez-Ramos, M. & Bongers, F. (2015). Biomass is the main driver of changes in ecosystem process rates during tropical forest succession. *Ecology*, 96, 1242–1252.

Malhi, Y., Silman, M., Salinas, N., Bush, M., Meir, P. & Saatchi, S. (2010). Introduction: Elevation gradients in the tropics: laboratories for ecosystem ecology and global change research. *Glob. Change Biol.*, 16, 3171–3175.

Malhi, Y., Doughty, C. & Galbraith, D. (2011). The allocation of ecosystem net primary productivity in tropical forests. *Phil. Trans. R. Soc. B*, 366, 3225–3245.

Malhi, Y., Girardin, C.A.J., Goldsmith, G.R., Doughty, C.E., Salinas, N., Metcalfe, D.B. *et al.* (2017a). The variation of productivity and its allocation along a tropical elevation gradient: a whole carbon budget perspective. *New Phytol*, doi:10.1111/nph.14189, press.

Malhi, Y., Shenkin, A., Patrick-Bentley, L., Salinas, N., Blonder, B., Goldsmith, G.R. *et al.* (2017b) Relating plant canopy traits and ecosystem function at multiple scales in tropical forests: the CHAMBASA project, In preparation.

Marino, G., Aqil, M. & Shipley, B. (2010). The leaf economics spectrum and the prediction of photosynthetic light–response curves. *Funct. Ecol.*, 24, 263–272.

Moorcroft, P.R., Hurtt, G.C. & Pacala, S.W. (2001). A method for scaling vegetation dynamics: the ecosystem demography model (ed). *Ecol. Monogr.*, 71, 557–586

Nemani, R.R., Keeling, C.D., Hashimoto, H., Jolly, W.M., Piper, S.C., Tucker, C.J. *et al.* (2003). Climate-driven increases in global terrestrial net primary production from 1982 to 1999. *Science*, 300, 1560–1563.

Nottingham, A.T., Turner, B.L., Whitaker, J., Ostle, N.J., McNamara, N.P., Bardgett, R.D. et al. (2015). Soil microbial nutrient constraints along a tropical forest elevation gradient: a belowground test of a biogeochemical paradigm. *Biogeosciences*, 12, 6071–6083.

Poorter, L., Wright, S.J., Paz, H., Ackerly, D.D., Condit, R., Ibarra-Manríquez, G. et al. (2008). Are functional traits good predictors of demographic rates? evidence from five neotropical forests. *Ecology*, 89, 1908–1920.

Purves, D. & Pacala, S. (2008). Predictive models of forest dynamics. *Science*, 320, 1452–1453.

Quesada, C.A., Phillips, O.L., Schwarz, M., Czimczik, C.I., Baker, T.R., Patiño, S. et al. (2012). Basin-wide variations in Amazon forest structure and function are mediated by both soils and climate. *Biogeosciences*, 9, 2203–2246.

Raich, J.W., Russell, A.E. & Vitousek, P.M. (1997). Primary productivity and ecosystem development along an elevational gradient on Mauna Loa, Hawai'i. *Ecology*, 78, 707–721.

Santiago, L.S., Kitajima, K., Wright, S.J. & Mulkey, S.S. (2004). Coordinated changes in photosynthesis, water relations and leaf nutritional traits of canopy trees along a precipitation gradient in lowland tropical forest. *Oecologia*, 139, 495–502.

Scheiter, S., Langan, L. & Higgins, S.I. (2013). Next-generation dynamic global vegetation models: learning from community ecology. *New Phytol.*, 198, 957–969.

Shenkin, A., Bentley, L.P., Oliveras, I., Salinas, N., Adu-Bredu, S., Marimon, B.H. et al. (2017). *Tropical Tree Crown Size and Shape across Biogeography*. Convergence and Variation. Ecological Monographs, under review, Ecosystems and Gradients.

Strigul, N., Pristinski, D., Purves, D., Dushoff, J. & Pacala, S. (2008). Scaling from trees to forests: tractable macroscopic equations for forest dynamics. *Ecol. Monogr.*, 78, 523–545.

Sundqvist, M.K., Sanders, N.J. & Wardle, D.A. (2013). Community and ecosystem responses to elevational gradients: processes, mechanisms, and insights for global change. *Annu. Rev. Ecol. Evol. Syst.*, 44, 261–280.

Tanner, E.V.J., Vitousek, P.M. & Cuevas, E. (1998). Experimental investigation of nutrient limitation of forest growth on wet tropical mountains. *Ecology*, 79, 10–22.

Vazquez, A.J. & Givnish, T.J. (1998). Altitudinal gradients in tropical forest composition, structure, and diversity in the Sierra de Manantlán. *J. Ecol.*, 86, 999–1020.

Walters, M.B. & Reich, P.B. (1999). Low-light carbon balance and shade tolerance in the seedlings of woody plants: do winter deciduous and broad-leaved evergreen species differ? *New Phytol.*, 143, 143–154.

van de Weg, M.J., Meir, P., Grace, J. & Atkin, O.K. (2009). Altitudinal variation in leaf mass per unit area, leaf tissue density and foliar nitrogen and phosphorus content along an Amazon-Andes gradient in Peru. *Plant Ecol. Divers*, 2, 243–254.

van de Weg, M.J., Meir, P., Grace, J. & Ramos, G.D. (2012). Photosynthetic parameters, dark respiration and leaf traits in the canopy of a Peruvian tropical montane cloud forest. *Oecologia*, 168, 23–34.

van de Weg, M.J., Meir, P., Williams, M., Girardin, C., Malhi, Y., Silva-Espejo, J. et al. (2014). Gross primary productivity of a high elevation tropical montane cloud forest. *Ecosystems*, 17, 751–764.

Wright, J.S. (2002). Plant diversity in tropical forests: a review of mechanisms of species coexistence. *Oecologia*, 130, 1–14.

Wright, I.J., Reich, P.B., Westoby, M., Ackerly, D.D., Baruch, Z., Bongers, F. et al. (2004). The worldwide leaf economics spectrum. *Nature*, 428, 821–827.

Wright, S.J., Kitajima, K., Kraft, N.J.B., Reich, P.B., Wright, I.J., Bunker, D.E. et al. (2010). Functional traits and the growth–mortality trade-off in tropical trees. *Ecology*, 91, 3664–3674.

Zimmermann, M., Meir, P., Bird, M.I., Malhi, Y. & Ccahuana, A.J.Q. (2010). Temporal variation and climate dependence of soil respiration and its components along a 3000 m altitudinal tropical forest gradient. *Global Biogeochem. Cycles*, 24, GB4012

## SUPPORTING INFORMATION

Additional Supporting Information may be found online in the supporting information tab for this article.